

Short communication

## Carbon deposition during propane dehydrogenation in a fuel cell

Yu Feng, Jing-Li Luo\*, Karl T. Chuang

Department of Chemical and Materials Engineering, University of Alberta, Edmonton, Alberta T6G 2G6, Canada

Received 27 January 2007; received in revised form 23 February 2007; accepted 23 February 2007

Available online 2 March 2007

### Abstract

Carbon deposition in a high temperature proton-conducting fuel cell for selective propane dehydrogenation to propylene with co-generation of electrical power was investigated. Comparison of carbon deposition was made for catalytic propane dehydrogenation under an open circuit condition and electro-catalytic conversion of propane to propylene on the anode catalyst of synthesized chromium(III) oxide during fuel cell operation conditions with current flow. Carbon deposition under the fuel cell operating conditions was much less than that under the open circuit conditions. Chromium(III) oxide catalyst modified by potassium showed a better resistance to carbon formation under the open circuit conditions but was similar to the unmodified catalyst under current flow conditions.

© 2007 Elsevier B.V. All rights reserved.

**Keywords:** Carbon deposition; Propane dehydrogenation; Chromium(III) oxide; Fuel cell

### 1. Introduction

Propane can be selectively dehydrogenated to propylene in a proton-conducting fuel cell [1–3]. In principle, propane is dehydrogenated to propylene, electrons and protons at the anode catalyst surface, and then protons conduct through the proton-conducting electrolyte to the cathode side, where they combine with oxygen and electrons to produce water; while electrons go through external circuit to produce electricity. This process has the unique advantage of obtaining *value-added product propylene and electric power* simultaneously. Our fuel cell group at the University of Alberta has proved the feasibility of conversion of propane to propylene in a proton-conducting fuel cell [1,2,4,5]. Although operating temperatures (550–700 °C) of the fuel cell benefited the kinetics of propane dehydrogenation, carbon deposition during the process became a problem at these temperatures, as the carbon poisoned the anode catalysts leading to their deactivation and deterioration of the product distribution.

High temperature dehydrogenation reactions are relatively unselective because all equivalent C–H bonds have an equal bonding energy, and therefore an equal chance of reacting [6]. Propylene is formed when two C–H bonds of neighboring carbons are broken and a C=C double bond is formed. If the two C–H bonds are part of two different propane molecules, higher molecular-weight hydrocarbons are formed, and extensive C–H bond breaking and C–C bond formation may lead to hydrogen gas and coke. Hence, it is clear that a proper choice of catalyst is needed to achieve an optimum dehydrogenation process that has both high conversion and high selectivity to propylene.

Since the pioneering work of Frey et al. [7], the superior properties of supported chromium oxide catalysts for alkane dehydrogenation are well-known, and Cr<sub>2</sub>O<sub>3</sub>/Al<sub>2</sub>O<sub>3</sub> catalysts are widely used in industrial processes [8–10]. A possible catalytic mechanism for alkane dehydrogenation over Cr<sub>2</sub>O<sub>3</sub>/Al<sub>2</sub>O<sub>3</sub> catalysts, illustrated in Fig. 1 [11], involves the adsorption of an alkane on a coordinative unsaturated Cr<sup>3+</sup>-center, which can be either isolated or clustered. In a second step, the C–H bond of the alkane is broken, and an O–H bond and a Cr–H bond are formed. In the product formation step, an alkene is released from the surface. The catalytic surface is regenerated by the formation of H<sub>2</sub>. In this study, chromium(III) oxide was selected as the anode catalyst in fuel cell to investigate

\* Corresponding author at: #536, Department of Chemical and Materials Engineering, University of Alberta, Edmonton, Alberta T6G 2G6, Canada. Tel.: +1 780 492 2232; fax: +1 780 492 2881.

E-mail address: [jingli.luo@ualberta.ca](mailto:jingli.luo@ualberta.ca) (J.-L. Luo).

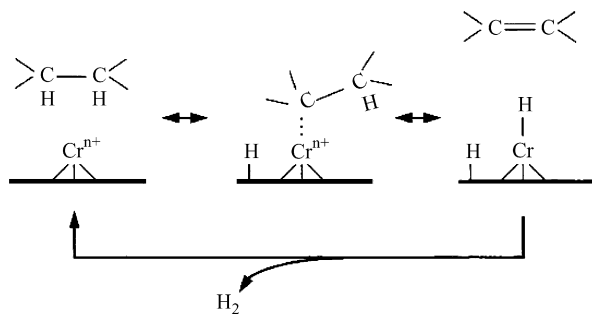


Fig. 1. Possible catalytic mechanism for alkane dehydrogenation over  $\text{Cr}_2\text{O}_3/\text{Al}_2\text{O}_3$  catalysts.

the carbon deposition behavior during the process of propane dehydrogenation.

## 2. Experimental

### 2.1. Synthesis of chromium(III) oxide

The sol-gel method was used to synthesize nano-chromium oxide dehydrogenation catalysts. A  $0.18 \text{ mol L}^{-1} \text{ Cr}^{3+}$  aqueous solution was prepared by dissolving  $\text{Cr}(\text{NO}_3)_3 \cdot 9\text{H}_2\text{O}$  (Aldrich; 99% purity) in deionized water. The catalyst precursor was formed by precipitation from this solution with an approximately  $2 \text{ mol L}^{-1}$  ammonia aqueous solution added dropwise with stirring by a Teflon-coated magnetic stir bar. The reacting mixtures were stirred continuously throughout the synthesis procedure. Base was added until the solution became slightly basic, as indicated by pH paper. The precipitate was separated by filtration, washed several times with deionized water, and then suspended in 2-butanol. The resulting gel was stirred overnight. When gelation was complete, the solute initially present was contained within the final gel. The green gelatinous substance formed was filtered again. The obtained material was sintered in an oven by  $1^\circ\text{C min}^{-1}$  to  $110^\circ\text{C}$  where it was kept for 2 h and then the temperature was increased by  $2^\circ\text{C min}^{-1}$  to  $600^\circ\text{C}$ , at which it was kept for 6 h.

Since chromium(III) oxide is not electronically conductive at high temperatures, it cannot be used alone as a fuel cell electrode. To increase the electronic conductivity of the catalyst, conductive Ag-paste was admixed with chromium(III) oxide by volume ratio 50:50 for testing. Two kinds of  $\text{Cr}_2\text{O}_3$  based anode catalysts were prepared for testing: (1)  $\text{Cr}_2\text{O}_3 + \text{Ag}$  (50:50) and (2)  $\text{Cr}_2\text{O}_3 + \text{Ag}$  (50:50) modified by addition of 0.5% (wt%) potassium through pre-treating  $\text{Cr}_2\text{O}_3 + \text{Ag}$  with potassium hydroxide solution.

### 2.2. Fuel cell system

A vertical fuel cell set-up with a glass sealant was adopted to ensure good anode side gas seal [12], as shown in Fig. 2. This system comprised anode and cathode compartments, each consisting of two co-axially aligned alumina tubes. The inner tube extended from outside the heated reaction zone to a position close to the respective electrode of the cell. The two tubes were

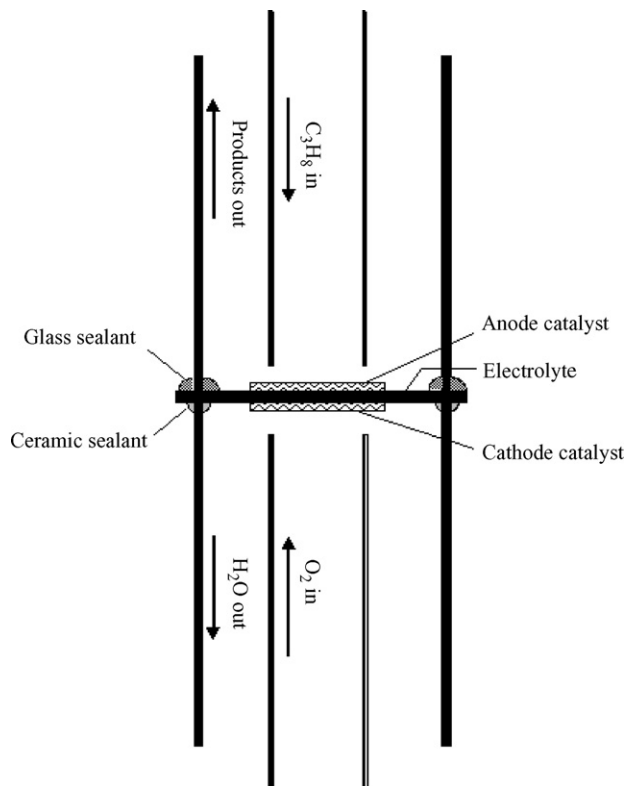


Fig. 2. Schematic of  $\text{C}_3\text{H}_8\text{-O}_2$  fuel cell set-up design.

fastened together at the remote end with a tailing gas outlet. The cell was sandwiched between the outer tubes of the anode and cathode compartment. The outer perimeter of anode and cathode outer tubes was sealed to the cell by applying a thin layer of glass and ceramic sealant (Aremco 503), respectively. Platinum gauze (52 mesh) was applied as the current collector for both anode and cathode.

The assembled cell was placed in a tubular furnace (Thermolyne F79300) having a uniform temperature zone:  $\pm 0.6^\circ\text{C}$  over the thermal couple measurement point 3.54 cm length of the cell. The seals were cured gradually as the cell was heated to the prescribed temperature for testing [12], prior to operation of the cell under reaction conditions. During the heating procedure, nitrogen passed through the anode chamber and air through the cathode chamber.

All the fuel cell experiments were carried out in the temperature range of  $550\text{--}700^\circ\text{C}$ . After the cell had stabilized at the operating temperature, the anode feed was switched to pure  $\text{C}_3\text{H}_8$  (Praxair, grade 2.0).  $\text{O}_2$  (Praxair, grade 2.6) was supplied to the cathode side as oxidant via the inner tube. The gas flow rates were carefully controlled with mass flow controllers.

### 2.3. Electrolyte

Fifteen percent Y-doped  $\text{BaCeO}_3$  (BCY15) was used as the proton-conducting electrolyte. The preparation procedure was described in the previous report [2]. Briefly Y-doped  $\text{BaCeO}_3$  powder was prepared from  $\text{BaCeO}_3$ ,  $\text{CeO}_2$  and  $\text{Y}_2\text{O}_3$  by solid-state reactions, and then solid disks of electrolyte were made by pressing the powder and sintering at high temperature.

## 2.4. Electrodes

The anode and cathode were prepared by screen-printing  $\text{Cr}_2\text{O}_3 + \text{Ag}$  paste and platinum paste (Heraeus CL11-5100), respectively, onto the corresponding surfaces of the BCY15 electrolyte disk, and then were dried in air at  $120^\circ\text{C}$  for 30 min to remove the organic solvent and to increase adhesion to the electrolyte.

## 2.5. Characterization of anode catalysts

The microstructure of the synthesized chromium(III) oxide powder was examined using a Hitachi S-2700 scanning electron microscope (SEM). Freshly prepared and used  $\text{Cr}_2\text{O}_3 + \text{Ag}$  anodes from the  $\text{C}_3\text{H}_8\text{-O}_2$  fuel cell before and after test were compared using X-ray powder diffraction (XRD) analysis. Carbon deposits on anode catalysts were characterized with X-ray photoelectron spectroscopy (XPS) and energy dispersive X-ray spectrometry (EDX) techniques. Before analysis by XPS or EDX, the sample of used anode catalyst was treated in Ar at  $400^\circ\text{C}$  for 10 h to remove the unreacted propane and other hydrocarbon species adsorbed on the anode.

## 3. Results and discussion

### 3.1. Materials

SEM micrograph (Fig. 3) of the chromium(III) oxide powder synthesized by sol-gel method showed the uniform distribution of particle size, mostly in the range of 250–350 nm. The XRD profiles of  $\text{Cr}_2\text{O}_3 + \text{Ag}$  before and after test in the fuel cell for 24 h (Fig. 4) showed no obvious changes in the anode material, and so the anode material prepared using this chromium(III) oxide powder was stable for use in the fuel cell for propane dehydrogenation.

### 3.2. Carbon deposition under open circuit conditions

Under the open circuit conditions the reactions taking place in the fuel cell chamber were those of thermal cracking and

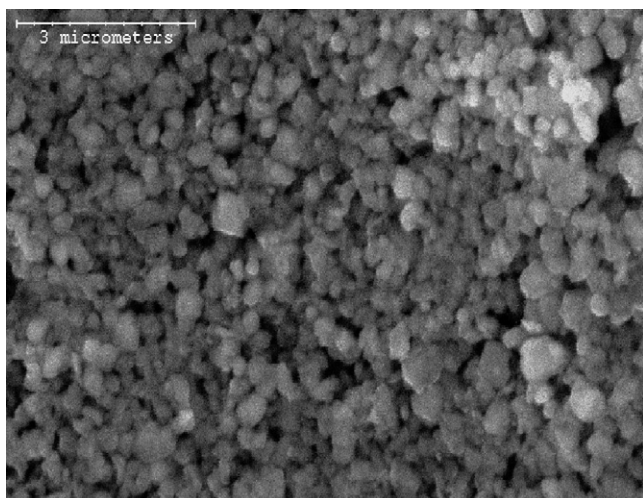


Fig. 3. Microstructure of synthesized chromium oxide powder.

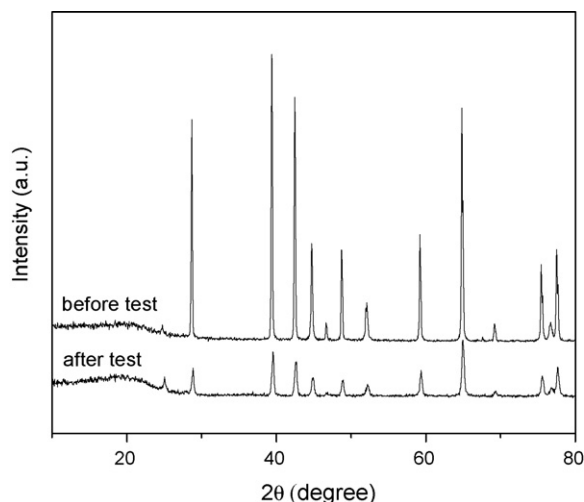


Fig. 4. XRD profiles of the anode  $\text{Cr}_2\text{O}_3 + \text{Ag}$  before and after test in fuel cell at  $700^\circ\text{C}$  for 24 h.

some other catalytic reactions occurring at the anode (Fig. 5). The gas components ( $\text{CH}_4$ ,  $\text{C}_2\text{H}_4$ ,  $\text{C}_2\text{H}_6$ ,  $\text{C}_3\text{H}_6$ ) arising from the thermal reactions [1,2] are thermodynamically favoured to form carbon on the anode catalyst in an irreversible process (Fig. 6). The thermodynamic bias to carbon deposition was very strong, especially at high temperatures, for propane, propylene and ethylene, and favored carbon deposition during propane dehydrogenation in the fuel cell at the operating temperatures ( $550\text{--}700^\circ\text{C}$ ). However, the rate of carbon formation was determined by the operating conditions and catalysts. Fig. 7 shows the carbon deposition from thermal cracking reactions in the fuel cell chamber with pure propane as feed. The carbon selectivity from thermal cracking of propane was dependent on the operating temperature and propane flow rate, i.e. contact time. Decreasing the operating temperature and reaction time diminishes carbon formation, but it must be prudent to do so because low temperatures are kinetically unfavorable while short reaction time causes low propane conversion. Generally the thermal reactions occurring in the hollow tube set-up (Fig. 5) make no significant contribution to carbon deposition on the catalyst but deteriorate gas products distribution thus decreasing propylene selectivity. So the carbon deposition caused by thermal reactions can be minimized through optimizing fuel cell set-up design.

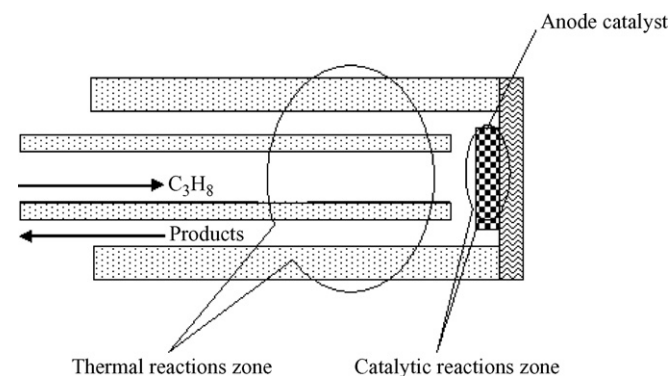


Fig. 5. Reaction zones in the anode chamber of fuel cell under open circuit conditions.

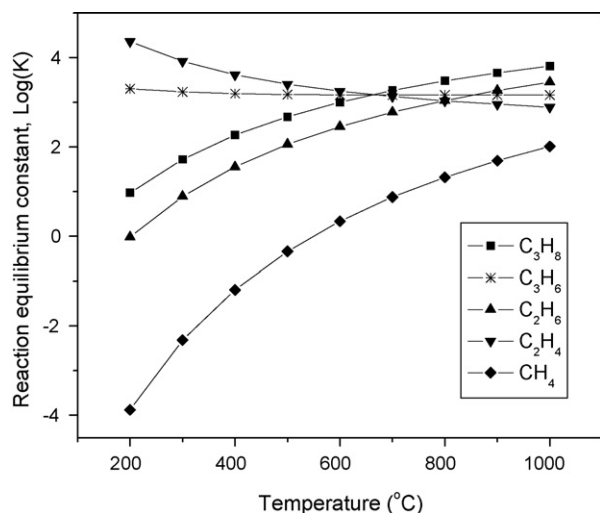


Fig. 6. Reaction equilibrium constants for carbon formation reaction from hydrocarbon species in the fuel cell chamber.

The behaviour leading to carbon deposition on the anode catalysts were investigated at 650 °C with propane flow rate of 60 ml min<sup>-1</sup> under open circuit conditions. Fig. 8 shows the XPS analysis of carbon on the Cr<sub>2</sub>O<sub>3</sub> based anode surfaces after testing in the fuel cell for 10 h. For comparison, Cr<sub>2</sub>O<sub>3</sub> + Ag anode catalyst and Cr<sub>2</sub>O<sub>3</sub> + Ag modified by addition of 0.5% potassium were also analyzed. It was found that carbon deposited occurred on both anode surfaces, but much more carbon was formed on the unmodified anode catalyst Cr<sub>2</sub>O<sub>3</sub> + Ag. The difference is due to the addition of potassium to the catalyst that modified the surface of chromium(III) oxide. Studies [13–15] showed that the catalytic properties of the chromium-based catalysts for dehydrogenation are due to surface Cr<sup>III</sup> species, and addition of potassium could sacrifice Cr<sup>III</sup> by formation of Cr<sup>VI</sup> containing compounds (K<sub>2</sub>CrO<sub>4</sub> or K<sub>2</sub>Cr<sub>2</sub>O<sub>7</sub> species). So the addition of potassium decreased the activity of chromium-based catalyst, i.e. the surface acidity, especially for the sites with strong acid-

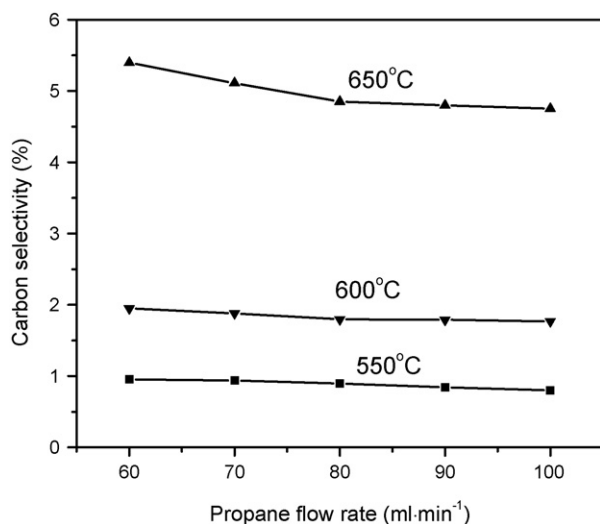


Fig. 7. Carbon selectivity from thermal cracking of propane in the fuel cell chamber.

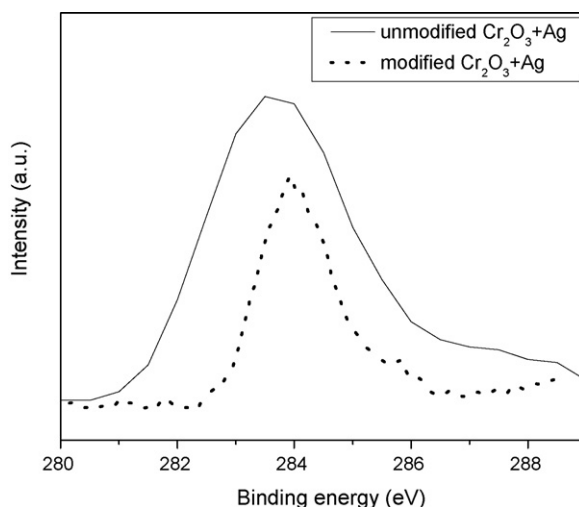


Fig. 8. Comparison of binding energy peak of C1s for different catalysts after 10 h fuel cell operation.

ity which tends to cause carbon deposition during the reaction. Our results are inconsistent with those studies.

### 3.3. Carbon deposition under fuel cell operation conditions

During the current flow conditions, the reaction process on the anode catalyst can be completely changed from chemical to electrochemical and thus the species formed on the catalyst surface readily reacted further to form products and generate power. Compared to the open circuit condition, much less carbon formation was detected on the chromium(III) oxide-based anode catalysts under the operating conditions by XPS technique (Fig. 9), which was confirmed by EDX analysis (Fig. 10). For the fuel cell continuously running at 650 °C for 10 h with a 50 mA current flow, the amount of carbon deposition on the anode catalyst Cr<sub>2</sub>O<sub>3</sub> + Ag was below 5% mass concentration in the catalyst, which corresponded to about 0.2% carbon selectivity based on the mass balance and carbon atom balance of

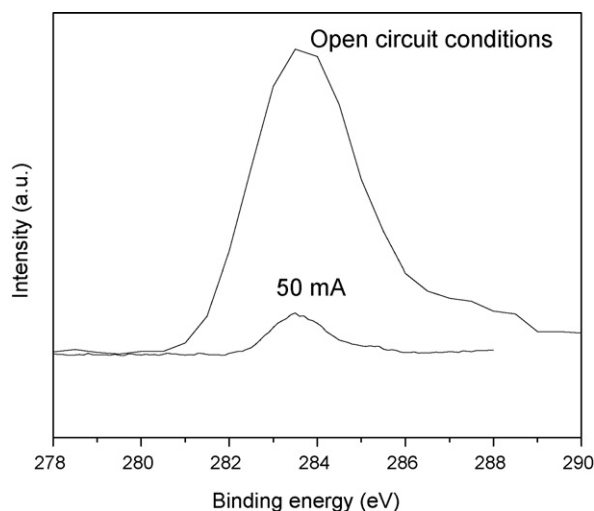


Fig. 9. Binding energy peaks of C1s under open circuit condition and at the current of 50 mA after 10 h fuel cell test.

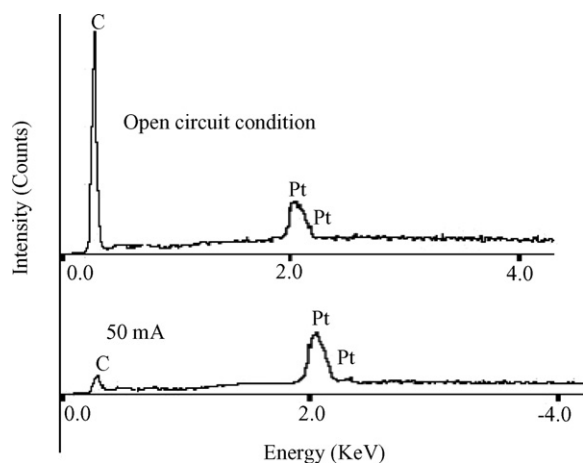


Fig. 10. EDX analysis of carbon deposition of anode catalyst  $\text{Cr}_2\text{O}_3 + \text{Ag}$  under open circuit condition and at the current of 50 mA after 10 h fuel cell tests.

inlet and outlet gas. In addition, the carbon deposition process at different currents was also monitored at the propane flow rate of  $50 \text{ ml min}^{-1}$  and operating temperature of  $600^\circ\text{C}$  (Fig. 11). Compared to open circuit conditions (i.e. zero current), the selectivity to carbon dropped steadily with increasing current. Thus, operating the fuel cell under current flowing conditions could obviously reduce the rate of carbon formation. This phenomenon may be due to the presence of electrons distribution on the anode catalyst under current flow conditions. The electrons on the anode catalyst formed a local electrical field which could influence the reaction mechanism of propane dehydrogenation, and enable the gas products species of propylene and small amounts of other by-products to be easily desorbed before they could be further dehydrogenated to form carbon. In contrast, during the process of catalytic propane dehydrogenation the gas species of propylene or other intermediate are difficult to be desorbed and contributed to carbon deposition [3]. Because there are no other publications available on the propane dehydrogenation process in a proton-conducting fuel cell, the details of carbon deposition mechanism during

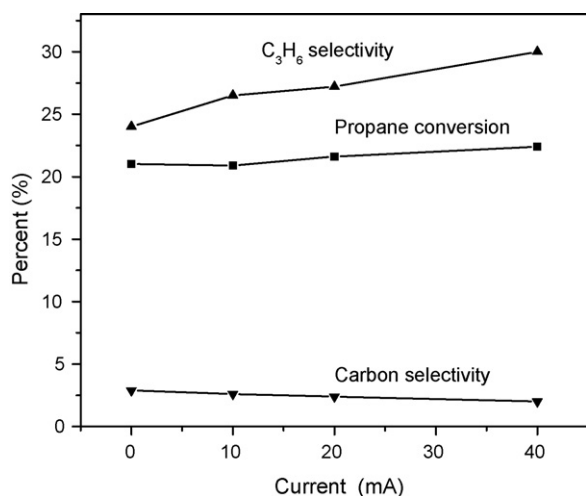


Fig. 11. Propane conversion and selectivities to carbon and propylene as functions of applied current (temperature,  $600^\circ\text{C}$ ; propane flow rate,  $50 \text{ ml min}^{-1}$ ).

this process are not yet understood and still under study in our group.

However, no obvious difference in carbon deposition was found for the modified and unmodified chromium(III) oxide under the current flowing conditions. The similarity may be due to the following reason: the surface chemistry of chromium oxide, such as the ratio of  $\text{Cr}^{\text{VI}}/\text{Cr}^{\text{III}}$ , was influenced by the local electrical field over the anode catalyst under the current flowing conditions; and this process probably is similar to the effect of addition of potassium to chromium oxide, which could reduce the strength of acid sites accounting for carbon deposition; but the effect of potassium was less pronounced when compared to the local electrical field, and thus was covered under the current flow conditions. As a consequence, the two anode catalysts showed almost the same ability to resist carbon deposition.

#### 4. Conclusions

Carbon deposition caused by thermal reactions occurring in hollow experimental fuel cell set-up was thermodynamically favorable but it deteriorated the gas products distribution. But the carbon formed on the anode due to catalytic or electrochemical reactions could poison the catalysts leading to the loss of their activity for dehydrogenation. Under current flow conditions by activating electrochemical reaction of propane dehydrogenation, the presence of local electrical field on the anode catalyst could suppress carbon deposition process, in contrast to the catalytic reactions under open circuit conditions. As a result, current flowing in the fuel cell dramatically inhibited the carbon deposition on the anode catalyst compared to open circuit conditions.

#### Acknowledgment

This work was supported by AERI/WED/WEPA.

#### References

- [1] Y. Feng, J. Luo, S. Wang, J. Melnik, K.T. Chuang, in: D. Ghosh (Ed.), Proceedings of the International Symposium on Fuel Cell and Hydrogen Technologies, Calgary, Canada, August 21–24, 2005, pp. 461–471.
- [2] Y. Feng, J. Luo, K.T. Chuang, *Fuel* 86 (2007) 123–128.
- [3] C.K. Cheng, Masters Thesis, University of Alberta, 2004, pp. 120–129.
- [4] Y. Feng, J. Luo, K.T. Chuang, *J. Electrochem. Soc.* 153 (2006) A1049–A1052.
- [5] Y. Feng, J. Luo, K.T. Chuang, *J. Electrochem. Soc.* 153 (2006) A865–A868.
- [6] H. Iwahara, H. Uchida, K. Morimoto, *J. Electrochem. Soc.* 137 (1990) 462–465.
- [7] F.E. Frey, R.D. Snow, W.F. Huppke, US Patent, No. 2349160 19440516, 1944.
- [8] M. Cherian, M.S. Rao, W.T. Yang, J.M. Jehng, *Appl. Catal. A* 233 (2002) 1–33.
- [9] W.K. Jozwiak, W. Ignaczak, D. Dominiak, T.P. Maniecki, *Appl. Catal. A* 258 (2004) 33–45.
- [10] A. Tsyganok, P.J.E. Harlick, A. Sayari, *Catal. Commun.* 8 (2007) 850–854.
- [11] B.M. Weckhuysen, R.A. Schoonheydt, *Catal. Today* 51 (1999) 223–232.
- [12] Y. Feng, J. Luo, K.T. Chuang, *J. New Mater. Electrochem. Syst.*, in press.
- [13] E. Rombi, M.G. Cutrufello, V. Solinas, S. De Rossi, G. Ferraris, A. Pistone, *Appl. Catal. A* 251 (2003) 255–266.
- [14] H.A. Mcveigh, Ph.D. Dissertation, University of Delaware, 1972, pp. 200–250.
- [15] I. Dybkjaer, A. Bjorkman, *Adv. Chem. Series* 109 (1972) 219–222.